Published in final edited form as:
J Immunol. 2014 November 15; 193(10): 5327–5337. doi:10.4049/jimmunol.1400201.

CXCL12/CXCR4 Blockade by Oncolytic Virotherapy Inhibits Ovarian Cancer Growth by Decreasing Immunosuppression and Targeting Cancer Initiating Cells[1]

Margaret Gil[*,2], **Marcin P. Komorowski**[*,2,3], **Mukund Seshadri**[§], **Hanna Rokita**[¶], **A. J Robert McGray**[†], **Mateusz Opyrchal**[**], **Kunle O. Odunsi**[†], and **Danuta Kozbor**[*,4]

[*]Department of Immunology, Roswell Park Cancer Institute, Buffalo, NY 14263 [§]Department of Pharmacology and Therapeutics, Roswell Park Cancer Institute, Buffalo, NY 14263 [†]Department of Gynecology, Roswell Park Cancer Institute, Buffalo, NY 14263 [**]Department of Medicine, Roswell Park Cancer Institute, Buffalo, NY 14263 [¶]Faculty of Biochemistry, Biophysics, and Biotechnology, Jagiellonian University, Kraków, Poland

Abstract

Signals mediated by the chemokine CXCL12 and its receptor CXCR4 are involved in progression of ovarian cancer by enhancing tumor angiogenesis and immunosuppressive networks that regulate dissemination of peritoneal metastasis and development of cancer initiating cells (CICs). Here, we investigated the antitumor efficacy of a CXCR4 antagonist expressed by oncolytic vaccinia virus (OVV) against an invasive variant of the murine epithelial ovarian cancer cell line ID8-T. This variant harbors a high frequency of CICs that form multilayered spheroid cells and express the hyaluronan receptor CD44 as well as stem cell factor receptor CD117 (c-kit). Using an orthotopic ID8-T tumor model, we observed that intraperitoneal delivery of a CXCR4 antagonist-expressing OVV led to reduced metastatic spread of tumors and improved overall survival over that mediated by oncolysis alone. Inhibition of tumor growth with the armed virus was associated with efficient killing of CICs, reductions in expression of ascitic CXCL12 and VEGF, and decreases in intraperitoneal numbers of endothelial and myeloid cells as well as plasmacytoid dendritic cells (pDCs). These changes, together with reduced recruitment of T regulatory cells, were associated with higher ratios of IFN-γ^+/IL-10^+ tumor-infiltrating T lymphocytes as well as induction of spontaneous humoral and cellular antitumor responses. Similarly, the CXCR4 antagonist released from virally-infected human CAOV2 ovarian carcinoma cells inhibited peritoneal dissemination of tumors in SCID mice leading to improved tumor-free survival in a

[1]This work was supported in part by the National Institutes of Health grants CA164475 and CA140886 (D.K.); an Anna-Maria Kellen Clinical Investigator Award of the Cancer Research Institute and RPCI-UPCI Ovarian cancer SPORE P50CA159981-01A1 (KO); the Roswell Park Alliance Foundation; and utilized Shared Resources supported by RPCI's Cancer center Support Grant P30CA06156 (Trump, DL).

[4]Address correspondence and reprint requests to Danuta Kozbor, Department of Immunology, Roswell Park Cancer Institute, Elm and Carlton Streets, Buffalo, NY 14263. Phone: 716-845-8668; Fax: 716-845-8906; danuta.kozbor@roswellpark.org.
[2]M.G. and M.P.K. contributed equally to this work.
[3]Current address: Department of Virology, National Institute of Public Health-National Institute of Hygiene, 24 Chocimska Street, 00-791 Warsaw, Poland

Disclosures
The authors have no financial conflict of interest.

xenograft model. Our findings demonstrate that OVV armed with a CXCR4 antagonist represents a potent therapy for ovarian CICs with a broad antitumor repertoire.

Introduction

Epithelial ovarian carcinoma (EOC) is the leading cause of death from gynecological malignancies (1). Peritoneal dissemination is a common route of disease progression of ovarian cancer, which occurs by implantation of tumor cells onto the mesothelial lining in the peritoneal cavity (2, 3). Despite modest improvement in progression-free and median survival using adjuvant platinum and paclitaxel chemotherapy following cytoreductive surgery, overall survival rates for patients with advanced EOC remain disappointingly low (4). Preclinical and clinical studies suggest that tumor initiation and maintenance are attributed to a unique population of “sphere-forming cells” enriched in cancer initiating cells (CICs) that critically contribute to ovarian cancer tumorigenesis, metastasis and chemotherapy resistance (5, 6). The presence of CICs in ovarian tissue samples and cell lines has been demonstrated by multiple studies (7–9), and several markers have been used for their identification including CD117, CD44, CD133, aldehyde dehydrogenase isoform 1 (ALDH1), and in some cases CD24 (9–11). These CICs have been shown to survive conventional chemotherapies and give rise to more aggressive, recurrent tumors (12). It is therefore important to develop therapies that simultaneously target CICs and the ovarian tumor microenvironment that promotes their growth. It is imperative that such strategies stimulate antitumor immune responses to durably extend remission rates since the presence of intraepithelial $CD8^+$-infiltrating T lymphocytes and a high $CD8^+$/regulatory T cell ratio have been associated with improved survival in patients with ovarian tumors (13–15).

Although the signals generated by the tumor microenvironment that regulate CICs are not fully understood, recent studies provide strong evidence for the role of the chemokine receptor CXCR4 in CIC maintenance, dissemination, and consequent metastatic colonization (16–19). Signals mediated by the CXCL12/CXCR4 axis are centrally involved in EOC progression as CXCL12 can stimulate ovarian cancer cell migration and invasion through extracellular matrix as well as DNA synthesis and establishment of a cytokine network in situations that are suboptimal for tumor growth (20). CXCL12 produced by tumor tissue and surrounding stroma stimulates VEGF-mediated angiogenesis (21) and the recruitment of endothelial progenitor cells from the bone marrow (22, 23). CXCL12 has also been shown to recruit suppressive $CD11b^+Gr1^+$ myeloid cells and pDCs at tumor sites (24–26), and induce intratumoral T regulatory cells (Tregs) localization (26, 27), which impede immune mechanisms of tumor destruction. Therefore, modulation of the CXCL12/CXCR4 axis in ovarian cancer could impact multiple aspects of tumor pathogenesis including immune dysregulation. Several CXCR4 antagonists have demonstrated antitumor efficacy in preclinical models and have been evaluated in early clinical trials (28–31). However, given the abundant expression of CXCR4 by many cell types including those of the central nervous, gastrointestinal, and immune systems (32), the side-effects of these antagonists need to be taken into consideration. Furthermore, the impact of soluble CXCR4 antagonists on the mobilization of CXCR4-expressing bone marrow (BM)-derived stem and progenitor

cells represents an additional concern, particularly when combined with chemotherapeutic agents, due to the potential for increased toxicity to hematopoiesis (33, 34).

To overcome some of these concerns related to the systemic delivery of soluble CXCR4 antagonists, we designed a tumor cell-targeted therapy that delivered a CXCR4 antagonist, expressed in the context of the murine Fc fragment of IgG2a via an oncolytic vaccinia virus (OVV-CXCR4-A-Fc) (35). To that end, the antagonist was cloned into the genome of OVV, where selective replication in cancer cells is associated with cellular EGFR/Ras signaling, thymidine kinase (TK) elevation and type-1 interferon resistance (36). We have chosen OVV as a delivery vector because the virus has evolved mechanisms for rapid cell-to-cell spread to distant tissues, strong lytic ability, large transgene-encoding capacity, and proven safety in humans as a vaccine (36–38). The destructive nature of a poxvirus infection results in the release of several cellular and viral danger signals leading to generation of inflammatory responses that ultimately overcome tumor-mediated immune suppression to clear the virus (35, 39, 40), while also mediating tumor destruction.

Previously, we have demonstrated that OVV-CXCR4-A-Fc delivered intravenously to mice with orthotopic breast tumors attains higher intratumoral concentration of the inhibitor than its soluble counterpart and OVV-CXCR4-A-Fc exhibits increased efficacy over that mediated by oncolysis alone (35). These results together with those of the previous studies showing targeting of lung and colon CICs (37) and breast cancer stem-like cells (41) with oncolytic vaccinia viruses prompted us to investigate whether OVV-CXCR4-A-Fc could effectively eliminate metastatic ovarian cancer dissemination and enhance the pool of tumor-associated antigens for immunization. Using a highly tumorigenic variant of the murine epithelial ovarian cancer cell line ID8-T that harbors $CD44^+$ and $CD117^+$ CICs, we demonstrated that antitumor efficacy of i.p.-delivered OVV-CXCR4-A-Fc was multifaceted resulting in a direct oncolysis of CICs, decreases in recruitment of suppressive elements promoting tumor vascularization, and stimulation of antitumor immunity monitored by the presence of humoral and cellular immune responses to Wilms' tumor antigen 1 (WT1) expressed by ID8-T cells.

Materials and Methods

Animals and Cell Lines

Female C57BL/6 and C.B-Igh-1b/IcrTac-Prkdc SCID mice, 6–8 wk of age, were obtained from the Taconic Farms (Hudson, NY) and the Laboratory of Animal Resources at Roswell Park Cancer Institute (RPCI, Buffalo, NY), respectively. Experimental procedures were performed in compliance with protocols approved by the Institutional Animal Care and Use Committee of the RPCI. ID8 mouse ovarian epithelial cells derived from spontaneous malignant transformation of C57BL/6 MOSE cells (42), whereas human CaOV2 cells derived from an ascitic tumor obtained from a patient suffering with a primary stage III serous ovarian carcinoma (43). Human $HuTK^-$ 143 fibroblasts, human cervical carcinoma HeLa cells (44), and African green monkey cell line CV-1 (45) were obtained from the American Type Culture Collection (ATCC, Manassas, VA).

Viruses

The pFU-Luc2-Tomato lentiviral vector encoding firefly luciferase (Luc) fused to the red fluorescent protein td-Tomato (L2T) was provided by Dr. M. Clarke, Stanford University, Stanford, CA. All vaccinia viruses used in this study are of the Western Reserve strain with disrupted thymidine kinase (*TK*) and vaccinia growth factor (*VGF*) genes for enhanced cancer cell specificity. The generation and characterization of vaccinia viruses expressing the enhanced green fluorescence protein (EGFP; OVV-EGFP) and OVV-CXCR4-A-Fc have been previously described (35). For the generation of OVV expressing Fc portion of murine IgG2a (OVV-Fc), the Fc fragment was obtained from pFUSE-mIgG2A-Fc2 vector (InvivoGen, San Diego, CA) and cloned into the *SalI* and *XbaI* restriction enzyme sites of the pCB023 plasmid under control of the vaccinia synthetic early/late promoter *Pse/I* (46). The inserted fragment was flanked by portions of *TK* gene that allowed for the homologous recombination of mFcIgG2a into the *TK* locus of parental VSC20 vaccinia virus. For these experiments, confluent wells of CV-1 cells were infected for 2 h at 37°C with 1.4×10^5 PFU of VSC20 in 1.0 ml of MEM-2.5% FCS. Supernatants were removed, and a liposomal transfection (Invitrogen, Carlsbad, CA) of pCB023-mFcIgG2a plasmid was performed according to manufacturer's protocol. Multiple plaques of the recombinant viruses were isolated on a monolayer of $HuTK^-$ 143 fibroblasts by BrdU selection. The OVV-CXCR4-A-Fc, OVV-EGFP and OVV-Fc viruses were amplified on HeLa cells, purified over a sucrose gradient, titrated, and used for *in vitro* and *in vivo* studies.

Self-renewal spheres formation assay and viral infection

The sphere assay was performed as described (12). Briefly, tumor cells were plated in ultra-low attachment plates (Corning Inc., Corning, NY) in serum-free Dulbecco's Modified Eagle's Medium/F12 supplemented with 5 μg/ml insulin (Sigma, St. Louis, MO), 0.4% bovine serum albumin (Sigma), 10 ng/mL basic fibroblast growth factor (Invitrogen), and 20 ng/mL recombinant epidermal growth factor (Invitrogen) at a density of 1,000 – 10,000 viable cells/well. Sphere formation was assessed 12–14 days after seeding. For the viral infection, spheres were collected by gentle centrifugation, dissociated in Trypsin-EDTA solution, and incubated with OVV-EGFP at a multiplicity of infection (MOI) of 1 for 2 h in 5% CO_2. Cells were washed, seeded in cultures and evaluated for EGFP expression by fluorescence microscopy after 12 h.

In vivo studies

Tumorigenicity of the bulk ID8 and ID8-T cell lines was assessed by measuring tumor formation after injection of different numbers of cells (2×10^4 - 5×10^6) s.c. into dorsal tissues or i.p. into C57BL/6 or SCID mice (n = 3 – 4 per group). In some experiments, ID8-T tumor cells were sorted based on CD44 and/or CD117 expression prior to s.c. inoculation of $CD44^+CD117^+$, $CD44^+CD117^-$, $CD44^-CD117^+$, and $CD44^-CD117^-$ cell populations (5×10^3 - 2×10^6 cells per injection in 50 μl PBS) into C57BL/6 mice. Engrafted mice were inspected biweekly for tumor appearance by palpation and subjected to bioluminescence imaging to quantify tumor burden using the Xenogen IVIS Imaging System (Perkin Elmer, Waltham, MA) after injection of 200 μl of Luciferin-D (150 mg/kg body weight, Biosynth International Inc., Itasca, IL). For oncolytic virotherapy studies, C57BL/6 mice (*n* = 8 – 10

per group) were injected i.p. with 5×10^5 ID8-T cells whereas SCID mice (n = 5 per group) were injected i.p. with 5×10^6 CaOV2 cells. Oncolytic virotherapy with OVV-CXCR4-A-Fc, OVV-Fc or OVV-EGFP (10^8 PFU delivered i.p.) was initiated 7 days later. Tumor progression was monitored by bioluminescence imaging. For experiments in CAOV2-challenged SCID mice, animals were treated with a lower titer of the virus (2.5×10^7 PFU) and vaccinia virus-specific antibodies (100 μg of antibodies with neutralizing titer of 1 : 100) were delivered 7 days after viral challenge to inhibit spreading infection as described (47). Control mice received PBS or UV-inactivated virus. At the end of the experimental period, tumor-bearing mice were sacrificed and organs were examined for tumor development and metastatic spread. Tumor and stromal cells were obtained from centrifuged cell pellets of ascites or peritoneal fluids collected from tumor-bearing mice after injection of 1 ml of PBS.

Flow Cytometry

ID8 and ID8-T tumor cells were analyzed by staining of single-cell suspension with rat mAbs against mouse CD117-APC, CD44-PerCP-Cy5.5, CD24-FITC, CD133-PE and CXCR4-PE, whereas human CaOV2 tumor cells were stained with mouse anti-human mAbs: CD44-PE and CD24-FITC (BD Pharmingen, San Jose, CA). Intracellular expression of WT1 was evaluated with anti-WT1 mAb (Santa Cruz Biotechnology, Santa Cruz, CA) followed by goat anti-mouse IgG-FITC (BD Pharmingen). All evaluations were performed on a FACScalibur flow cytometer (Becton Dickinson, Franklin Lakes, NJ). After gating on forward and side scatter parameters, at least 10,000 gated events were routinely acquired and analyzed using CellQuest software (Becton Dickinson Immunocytometry System). Sorting of $CD117^+CD44^+$, $CD117^+CD44^-$, $CD117^-CD44^+$ and $CD117^-CD44^-$ subsets of the ID8-T cell line was performed on a BD FACSAria flow cytometer (BD Biosciences, San Jose, CA). $ALDH1^+$ enzymatic activity was defined using the ALDEFLUOR kit (Stem Cell Technologies, Vancouver, BC, Canada) according to manufacturers' protocol.

The phenotypic analysis of tumor stromal cells and immune infiltrates (myeloid, endothelial cells, pDCs, Tregs and lymphocytes) were performed on single-cell suspensions prepared from peritoneal fluids collected at the time the control mice developed abdominal swelling. The cells were stained with rat anti-mouse mAbs: CD11b-APC, Ly6G-PE, Ly6C-FITC, B220-APC, CD11c-PE, CD45-APC-Cy7, VEGFR-2-PerCP-Cy5.5, CD34-FITC, CD4-PECy5, CD25-FITC, CD8-PECy5, IFN-γ-PE, IL-10-PE (BD Pharmingen), FoxP3-AlexaFluor 647 (eBioscience, San Diego, CA), and CD117-PE (Abcam, Cambridge, MA). The numbers of $CD4^+$ and CD8+ T cells expressing IFN-γ or IL-10 and $CD4^+$ T cells expressing FoxP3 were determined by intracellular staining using BD Cytofix/Cytosperm kit (BD Pharmingen) according to the manufacturer's protocol. Immune cells were gated on $CD45^+$ cells and endothelial progenitor cells were gated on $CD34^+$ cells for the analysis.

To determine the percent of $WT1_{126\text{-}134}/H\text{-}2D^b$ tetramer-specific $CD8^+$ T cells, lymphocytes obtained from axillary, brachial and inguinal lymph nodes were incubated with LPS-matured $WT1_{126\text{-}134}$ (RMFPNAPYL) peptide-coated DCs for 72 h in the presence of IL-2 (0.3 ng/ml) as described (48). The cells were washed and stained with rat anti-mouse CD8-PECy5 mAb and a PE-labeled $WT1_{126\text{-}134}/H\text{-}2D^b$ tetramer (MHC Tetramer

Production Facility, Baylor College of Medicine, Houston, TX). Background staining was assessed using isotype control antibodies (BD Pharmigen). Before specific antibody staining, cells were incubated with Fc blocker (anti-CD16/CD32 mAb) for 10 min. and analyzed on FACScalibur flow cytometer.

ELISA

The expression of CXCL12 and VEGF proteins in cell-free peritoneal fluids were analyzed by CXCL12/SDF-1α Elisa Quantikine kit (R&D System) and mouse VEGF Alpha Elisa kit (Antigenix America, Huntington Station, NY), respectively, according to the manufacturers' instruction. To measure the levels of WT1-specific antibodies after oncolytic virotherapy treatment, blood samples were collected by retro-orbital bleeding, and sera (1:100 dilution) were analyzed by ELISA with wells coated with 3 μg/ml of WT1 peptide (AAPPTec LLC., Louisville, KY).

CTL assay

Splenocytes were cultured with $WT1_{126\text{-}134}$ peptide -coated DCs at a 20:1 ratio for 24 h after which, cells were split and cultured in medium supplemented with murine rIL-2 (0.3 ng/ml) (BD Biosciences). The cytolytic activity of CTLs against ID8-T tumor cells was analyzed 5 days later by a standard 4-h ^{51}Cr-release assay. The percentage of specific lysis was calculated as follows: ([cpm experimental release - cpm spontaneous release]/[cpm maximum release cpm spontaneous release]) × 100. Maximum release was determined from the supernatants of cells that were lysed by the addition of 5% Triton X-100. Spontaneous release was determined from target cells incubated with medium only.

Statistical Analyses

The statistical significance of the difference between groups was performed using the two-tailed Student's *t* test assuming equal variance. Mixed model analysis of variance was used to compare differences in sphere formation, susceptibility of tumor cells to viral infection, metastatic dissemination, and immunosuppressive networks of the tumor microenvironment between groups. $P < 0.05$ was considered statistically significant. Kaplan-Meier survival plots were prepared and median survival times were determined for tumor-challenged groups of mice. Statistical differences in the survival across groups were assessed using the logrank Mantel-Cox method. Data were presented as arithmetic mean ± SD and analyzed using JMP (SAS Institute Inc., Cary, NC) on a Windows-based platform.

Results

Characterization of invasive ID8-T ovarian tumor cells

The invasive ID8-T tumor-forming variant was established from ascites of ID8 tumor-bearing C57BL/6 mice, after transduction with L2T lentiviral vector for the bioluminescence imaging purpose, based of expression of CIC-associated markers and aggressive growth characteristics. Flow cytometry analysis revealed that over 80% of ID8-T cells expressed the hyaluronan receptor CD44 in contrast to approximately 30% CD44-positive cells in the parental ID8 culture (Fig. 1A). The expression levels of the stem cell factor receptor CD117 (c-kit) and CD24 antigen were also higher on ID8-T cells, whereas numbers of cells positive

for CD133 antigen or exhibiting ALDH1 activity remained relatively low in both cultures (Fig. 1A). Cells positive for both CD44 and CD117 antigens comprised approximately 40% of ID8-T tumor, in contrast to less than 2% of these cells in ID8 culture, which contained mostly of $CD44^{-}CD117^{-}$ cells (Fig. 1B). Consistent with the previous report of CD44 and CD117 expression on sphere-forming ovarian CICs (11), the double-positive ID8-T cells or those expressing CD117 antigen were more efficient at sphere formation their CD117-negative counterparts (Fig. 1C). The bulk culture of ID8-T cells and its $CD44^{+}CD117^{-}$ subset had a reduced number and size of spheres, whereas the double-negative cells only sporadically formed spheres, suggesting that decreased numbers of $CD44^{+}CD117^{+}$ cells could be responsible for the low ability of sphere formation in the parental ID8 cell line (not shown).

Tumorigenicity of both bulk cultures as well as $CD44^{+}$ and/or $CD117^{+}$ subsets of ID8-T cells were examined by inoculating of exponentially smaller numbers of cells s.c. or into peritoneal cavities of C57BL/6 syngeneic and SCID mice. As shown in Table I, minimum of 5×10^{6} ID8 cells were required to initiate s.c. tumor growth in all inoculated mice within a 7-wk period, whereas injection of 10% of that number formed ID8-T tumors within much shorter period of time. ID8-T cells were also more efficient than their parental counterpart in developing bloody ascites in C57BL/6 and SCID mice with metastatic dissemination detected in the omentum, diaphragm, mesentery as well as peritoneal wall, indicating these cells recapitulate progression of ovarian cancer seen in patients. The rates of s.c. tumor formation with $CD44^{+}CD117^{+}$ and $CD44^{-}CD117^{+}$ tumor cells were consistently higher compared to the $CD117^{-}$ subset or the bulk culture (Table I). With injections of only 10,000 $CD117^{+}$ cells, palpable tumors were detected in all challenged mice within a 3-wk period. At this number and within the same period of time, the double-negative cells did not form tumor whereas $CD44^{+}CD117^{-}$ subset displayed an intermediate phenotype with lower tumorigenicity (Table I). Altogether, these results indicate that the ID8-T cell line is enriched for $CD44^{+}CD117^{+}$ and $CD117^{+}$ cells with CIC-like attributes compared to the parental ID8 culture.

Susceptibility of ID8-T tumor cells to vaccinia virus infection

We next investigated the susceptibility of both ID8 and ID8-T bulk cultures to OVV-EGFP infection (MOI = 1) by analyzing expression of EGFP in infected cells 12 h later. As shown in Fig. 2A, flow cytometry analysis revealed that numbers of $EGFP^{+}$ cells in ID8-T culture were almost twofold higher than those in the parental ID8 counterpart. Over 80% of infected cells were $CD44^{+}$ in both cultures but differed in CD117 expression. The latter antigen was present on approximately 40% of vaccinia virus-infected ID8-T cells, but was reduced almost to a background level in the ID8-infected culture (Fig. 2A). Results of this study suggest that the highly tumorigenic ID8-T cells are preferentially targeted by the virus. This observation was further supported by comparing OVV-EGFP infection in ID8-T adherent and spheroid populations. Analyses of both cultures under the fluorescence microscope revealed that though approximately half of the adherent ID8-T tumor cells were infected with the virus, the majority of spheroid cells were highly positive for EGFP expression (Fig. 2B).

To evaluate the ability of vaccinia virus to target ovarian CICs *in vivo* and any improvement in cancer cell killing gained through expression of the CXCR4 antagonist by the virus, ID8-T cells (5×10^5) were injected i.p. to syngeneic C57BL/6 mice and treated 7 days later with OVV-CXCR4-A-Fc or OVV-Fc at 10^8 PFU per injection. OVV-Fc rather than OVV-EGFP was used as a control vector for the *in vivo* studies to account for any possible effects that could be attributed to the Fc portion of the CXCR4-A-Fc fusion protein. The viruses were delivered i.p. and progression of tumor growth was quantified by bioluminescence imaging (radiance) 8 days after initiation of the treatment, which roughly corresponds to the termination of viral replication *in vivo* (not shown). As shown in Fig. 2C and D, the tumor burden after OVV-CXCR4-A-Fc treatment was significantly reduced compared to control and OVV-Fc-treated mice (Fig. 2D; $P = 0.007$ and $P = 0.015$, respectively), which was also reflected in lower numbers of tumor cells recovered from the peritoneal cavities of the treated mice (not shown). There were also phenotypic differences among tumor cells in control and virally-treated mice. As shown in Fig. 2E, percentages of $CD44^+CD117^+$ and $CD44^-CD117^+$ ID8-T cells were reduced almost to a background level after OVV-CXCR4-A-Fc treatment, and were significantly lower compared with those in OVV-Fc-treated mice ($P = 0.003$ and $P = 0.01$) and control animals ($P < 0.001$ and $P = 0.005$). The OVV-Fc treatment also reduced the numbers of $CD44^+CD117^+$ and $CD44^-CD117^+$ cells compared to the control tumor (Fig. 2E; $P < 0.05$), whereas both viruses were less effective in eliminating $CD44^+CD117^-$ and double-negative tumor cells. Because CXCR4 expression was present on the surface of $CD117^+$ sphere-forming cells (Supplemental Fig. 1), the higher *in vivo* reduction of $CD117^+$ CICs by OVV-CXCR4 compared to that in OVV-Fc-treated tumors might be attributed to an interference of the CXCR4-A-Fc antagonist, released from virally-infected cells, with the CXCL12/CXCR4 signaling axis on these cells and/or ADCC- and CDC-mediated killing (35). These findings, together with the increased percentage of the double-negative tumor cells in the virally-treated mice compared to controls ($P < 0.01$), suggets selective targeting of CICs by OVV-CXCR4-A-Fc *in vivo*.

OVV-CXCR4-A-Fc inhibits intraperitoneal dissemination of ID8-T tumor and improves overall survival

Although the single oncolytic virotherapy treatment led to significant reduction of tumor growth, the presence of residual tumors prompted us to examine whether additional injections of the virus, repeated twice in a weekly interval (Fig. 3A), would lead to improved overall survival. Figure 3B shows that OVV-CXCR4-A-Fc treatment resulted in an extended survival compared with control mice ($P < 0.001$) or animals treated with OVV-Fc ($P = 0.002$). At the time the control mice were sacrificed due to extensive tumor burden associated with the development of bloody ascites (Fig. 3C and D), the tumor load was significantly reduced in OVV-CXCR4-A-Fc-treated mice ($P = 0.005$) with no evidence of ascites production. These mice had also very small omental tumors and significantly reduced numbers of metastatic nodules (>5 mm) in the peritoneal cavities compared with control and OVV-Fc-treated counterparts (Fig. 3E; $P = 0.005$ and $P = 0.024$, respectively). In control mice, the metastatic nodules were present on the omentum as well as mesentery, diaphragm and peritoneal wall. At the time of the analysis, tumor growth in OVV-CXCR4-A-Fc-treated mice was restricted mainly to the omentum with sporadic metastatic lesions on diaphragm and peritoneal wall (Fig. 3F). The metastatic dissemination was more prominent after

treatment with OVV-Fc, though still lower than in the control mice ($P = 0.049$). Similar results were obtained using a xenograft model of the human CAOV2 ovarian carcinoma in SCID mice. Intraperitoneal injection of 2.5×10^7 PFU of OVV-CXCR4-A-Fc to CAOV2-bearing mice contributed to inhibition of tumor growth and metastatic dissemination leading to tumor-free survival in approximately 20% of CAOV2-bearing mice (Supplemental Fig. 2A, B).

OVV-CXCR4-A-Fc decreases levels of ascitic CXCL12 and VEGF as well as recruitment of EPCs, neutrophils/G-MDSCs and pDCs

Because the CXCR4 receptor for CXCL12 chemokine is one of the key stimuli involved in signaling between tumor cells and their microenvironment, we next investigated whether the inhibition of peritoneal dissemination of ID8-T tumor after targeting the CXCL12/CXCR4 signaling axis through an oncolytic virus would also result in changes within the tumor microenvironment. ELISA analyses of CXCL12 protein levels in peritoneal fluids harvested from tumor-bearing mice at the time when the control mice developed abdominal swelling consistent with ascites production, which roughly corresponded to 40 days after tumor challenge, revealed approximately four-fold higher levels of the chemokine in control and OVV-Fc-treated tumors compared with OVV-CXCR4-A-Fc counterparts (Fig. 4A; $P < 0.001$ and $P = 0.004$, respectively). Changes in CXCL12 expression paralleled those of VEGF whose ascitic levels were significantly reduced after treatment with the armed virus compared to control and OVV-Fc-treated tumors (Fig. 4B; $P < 0.001$). The latter factor, the expression of which is affected by CXCL12 (49), is pivotal in tumor angiogenesis (50, 51) and is associated with poor clinical outcome in patients with ovarian cancer (52). Thus, the higher CXCL12 and VEGF levels in peritoneal fluid together with intense neovascularization evidenced by an early sign of bloody ascites formation in OVV-Fc-treated tumors (Fig. 3C), suggests a potential angiogenic “rebound” in these mice compared to animals treated with OVV-CXCR4-A-Fc. This possibility was also supported by other findings, which demonstrated that binding of CXCL12 to CXCR4 expressed on circulating endothelial progenitor cells (EPCs), neutrophils/G-MDSCs, and pDCs triggers migration of these cells to the tumor sites (23–25, 53, 54).

Parallel analyses of the recruitment of EPCs to control and OVV-treated tumors examined by immunofluorescence staining of single-cell suspensions with mAbs specific for CD34, CD117, and VEGFR-2 revealed that the accumulation of EPCs in the peritoneal cavity after treatment with the armed virus was significantly diminished compared to control and OVV-Fc-treated counterparts (Fig. 4C; $P = 0.0009$ and $P = 0.013$, respectively). We also observed that the percentage of EPCs in control tumors was higher than that in OVV-Fc-treated mice ($P = 0.005$) despite comparable levels of CXCL12 and VEGF in both groups. Although the reason for this discrepancy is unknown, it is possible that other types of cells with proangiogenic activities including neutrophils/G-MDSCs and pDCs could be recruited to the tumor after infection with the unarmed virus promoting angiogenesis by producing VEGF and angiogenic cytokines, respectively (55, 56).

Because neutrophils/G-MDSCs are one of the first cell types recruited to the sites of infection (57), single-cell suspensions prepared from the control and virally-treated animals

were analyzed for the expression of CD11b, Ly6G and Ly6C markers by flow cytometry. We focused on cells with high expression of CD11b and Ly6G antigens and low Ly6C levels as this phenotype represents a population of granulocytes including neutrophils and G-MDSCs (58). Consistent with the notion that changes mediated by oncolytic virotherapy within tumors may act as a sink for activated neutrophils (59), the percentages of $CD11b^{+}Ly6C^{low}Ly6G^{+}$ cells in OVV-Fc-treated tumors were comparable with the controls (Fig. 4E) despite lower tumor burden (Fig. 3C). In contrast, the accumulation of neutrophils/G-MDSCs in OVV-CXCR4-A-Fc-treated tumors were significantly reduced compared to the control and OVV-Fc-treated counterparts (Fig. 4D; $P = 0.04$ and $P = 0.022$, respectively). A similar profile of responses were observed in the recruitment of $CXCR4^{+}$ pDCs ($B220^{high}Ly6C^{high}CD11c^{low}$), known to enhance tumor angiogenesis though production of IL-8 and TNF-α (56) and contribute to the tumor immunosuppressive network through induction of IL-10-expressing $CD8^{+}$ T cells (60). As migration of pDCs to the tumor sites is mediated by CXCL12 (25) and their expansion occurs during *in vivo* infection with vaccinia virus (61), the recruitment of pDCs in control and OVV-Fc-treated tumors were comparable and over three-fold higher than those in OVV-CXCR4-A-Fc-treated counterparts (Fig. 4E; $P = 0.004$ and $P = 0.01$, respectively). Altogether, these results suggest that the effect of virally delivered CXCR4 antagonist on the CXCL12/CXCR4 signaling axis prevails over the inflammatory capacity of the oncolytic virus in recruitment of neutrophils/G-MDSCs and pDCs to the tumor microenvironment.

Inhibition of tumor immunosuppressive networks by OVV-CXCR4-A-Fc is accompanied by the induction of antitumor immune responses

The inhibition of peritoneal dissemination of ID8-T tumor after OVV-CXCR4 treatment could be accounted for by both a direct cytotoxic effect of the virus as well as induction of antitumor immunity because of the ability of vaccinia virus to break Treg-mediated tolerance through Toll-like receptor (TLR)-dependent and -independent pathways (39, 40). This effect could be further augmented by release of the CXCR4-A-Fc fusion protein from OVV-CXCR4-A-Fc-infected tumor cells because CXCL12 induces intratumoral localization of $CD4^{+}CD25^{+}FoxP3^{+}$ Tregs in ovarian carcinoma (26, 27). In concordance with these findings, flow cytometry analysis revealed that treatment with OVV-CXCR4-A-Fc resulted in significantly lower percentages of tumor-infiltrating Tregs compared to control and OVV-Fc-treated tumors (Fig. 5A, $P = 0.001$ and $P = 0.03$, respectively). This could also contribute to significantly higher ratios of IFN-γ/IL-10-producing $CD4^{+}$ TILs in OVV-CXCR4-A-Fc-treated tumors compared to those in control ($P = 0.007$) and OVV-Fc-treated counterparts (Fig. 5B; $P = 0.048$). The changes were even more prominent with regard to the accumulation of IFN-γ-versus IL-10-producing $CD8^{+}$ TILs, reflected in over twofold increases in these ratios after OVV-CXCR4-A-Fc treatment than in control and OVV-Fc-treated mice (Fig. 5B; $P = 0.002$ and $P = 0.011$, respectively), suggesting that delivery of the armed virus is able to alter the inflammatory status of the tumor microenvironment in favor of immune activity over immune suppression.

To investigate whether the changes in the virally-treated tumor microenvironment were associated with the generation of spontaneous antitumor immunity, sera were collected from tumor-bearing mice before viral challenge and at the time of ascites development in control

mice. The sera specimens at dilution of 1:100 were analyzed by ELISA for the presence of antibodies to WT1 antigen as a surrogate marker of the treatment-induced antitumor immune responses. As shown in Fig. 5C, tumor-bearing control mice were unable to mount antitumor humoral responses. In contrast, WT1-specific serum antibodies were present in OVV-CXCR4-A-Fc-treated mice with approximately three-fold increases compared to those in OVV-Fc-treated counterparts (Fig. 5C; $P = 0.014$). The antibodies against WT1 were predominantly IgM with IgG detected in ~25% of OVV-CXCR4-A-Fc-treated mice with small tumor burden (not shown).

As new approaches for increasing the size and breadth of tumor-specific effector and memory pool of T cells are needed to enhance the efficacy of oncolytic virotherapy, we investigated the presence of oncolytic virotherapy-induced $CD8^+$ T cells to the $WT1_{126\text{-}134}$ epitope (RMFPNAPYL) with H2-D^b-binding motif in the same group of mice that were analyzed for humoral responses. To this end, cells isolated from the lymph nodes of control and virally-treated mice were examined for presence of $CD8^+$ T cells able to bind $WT1_{126\text{-}134}$/H2-D^b tetramers by a flow cytometric analysis after 72-h incubation with $WT1_{126\text{-}134}$ peptide-coated DCs. Figure 5D shows that the percentage of $CD8^+$ cells specific for $WT1_{126\text{-}134}$/H2-D^b epitope nearly doubled after OVV-CXCR4-A-Fc therapy compared to those in OVV-Fc-treated mice ($2.5 \pm 0.5\%$ vs. $1.6 \pm 0.3\%$; $P = 0.04$), whereas no $WT1_{126\text{-}134}$/H2-D^b tetramer-positive cells were detected in the control mice. Additionally, robust proliferation of splenocytes in response to stimulation with $WT1_{126\text{-}134}$ peptide-coated DCs was detected in cultures derived from tumor-bearing mice treated with OVV-Fc or OVV-CXCR4-A-Fc (data not shown). The proliferative responses were associated with the presence of antitumor CTL activities against ID8-T cells as monitored 5 days later by a standard 4-h ^{51}Cr-release assay (Fig. 5E).

Discussion

Ovarian CIC-mediated self-renewal, aggressive neovascularization, resistance to chemo- and radiotherapy, and marked local and systemic immunosuppression all contribute to current treatment inadequacy and tumor recurrence (9, 10). Thus, the curative potential of therapies against ovarian cancer hinges on eradicating CICs in addition to countering the tumor immunosuppressive network (62). Cancer stem cell identification was largely based on primary cells as well as early passage of cell lines in a mouse xenograft model (7, 11, 63). However, the majority of serum-cultured cell lines does not recapitulate the genotype and phenotype of ovarian cancer and therefore have limitations in regards to translating therapies to the clinic. The available immunocompetent EOC models to evaluate the multitude of therapies, especially those involving immunotherapy, relies primarily on ID8 cells (42) characterized by a slow growth rate and low numbers of CD117- and CD44-expressing cells. Therefore, the highly invasive ID8-T preclinical model described herein provides a means of investigating therapeutic impact on multiple aspects of ovarian cancer, including CICs, while also maintaining important pathophysiological characteristics of human ovarian tumors. Using this model, we have demonstrated that OVV-CXCR4-A-Fc treatment of mice challenged with ID8-T tumor resulted in reductions in intraperitoneal numbers of $CD44^+CD117^+$ and $CD44^-CD117^+$ CICs associated with increased survival. Specifically, we have shown that the armed oncolytic vaccinia virus was highly efficacious

in treating ID8-T tumor, and its multifaceted activities were associated with: (i) enhanced infection and killing of CICs, (ii) reduction of the tumor immunosuppressive network, and (iii) induction of antitumor humoral and cellular responses.

From a clinical perspective, our findings illustrating the contribution of OVV-CXCR4-A-Fc to targeting CICs as well as their supportive microenvironment may have significant therapeutic implications. *In vitro* analyses of tumor cells recovered from the peritoneal cavity after the therapy with OVV-CXCR4-A-Fc revealed almost complete depletion of $CD117^+CD44^+$ and $CD117^+CD44^-$ cells with the sphere-forming ability, though few of the remaining cells or $CD44^+CD117^-$ and double-negative subsets could account for subsequent tumor regrowth. For example, the $CD44^+CD117^-$ population with reduced viral clearance compared to CICs and “intermediate” ability to grow tumors at lower cell numbers could be responsible for the tumor recurrence. It is also possible that some ID8-T cells escaped the infection due to inadequate dissemination of the virus in the peritoneal cavity and/or the induction of anti-viral immunity, particularly after the second viral injection, that could neutralize the additional treatments (64). Alternatively, some tumor cells could be refractive to viral infection. Several lines of evidence indicate that CICs encompass progenitor and aneuploid populations of tumor cells with microenvironmentally-controlled switch between proliferation and quiescence (65–67). During the switch, quiescent CICs would undergo intermittent divisions leading to self-renewal and generation of proliferating progenitors that give rise to the bulk tumors as well as progenitor clones that constitute dormant subsets within tumor (65). Because cell cycle modifications are among the many mechanisms involved in controlling the dormant/CIC state of the tumor (65, 66), differences in cell cycle phases within euploid and aneuploid fractions may contribute to different susceptibility to vaccinia virus infection during the treatment. Thus, it becomes increasingly important to exploit the effect of the virally-delivered CXCR4 antagonist on the putative niche that nurtures CICs and their dormant progeny as a target for the oncolytic virotherapy.

Ovarian cancer is a heterogeneous disease with histologically defined subtypes, and reports have shown that CICs are involved in drug resistance and cancer recurrence (10), indicating that advances in oncolytic virotherapy require effective direct lysis of CICs and manipulation of the tumor microenvironment that contributes significantly to tumorigenesis (62). Although oncolytic viruses have great potential for the treatment of tumors, using direct cytotoxic and immune-stimulating mechanisms, and have progressed to phase III clinical trials in patients (68), there is a limited understanding of the viral interaction with different subsets of tumor cells as well as different elements of tumor stroma. In this study, we have demonstrated that targeting the CXCL12/CXCR4 migratory axis with the virally-expressed CXCR4 antagonist inhibited intratumoral accumulation of cancer-associated suppressive factors and cells including EPCs and immunosuppressive MDSCs, pDCs, Tregs as well as IL-10-producing $CD4^+$ and $CD8^+$ T cells, which had a significant therapeutic impact against metastatic dissemination of the tumor. Our findings also suggest that oncotherapy with the armed oncolytic vaccinia virus may enhance the induction of anti-CIC immune responses by increasing a pool of tumor-associated antigens released from the virally-infected CICs. In addition, because vaccinia virus-based vaccines have been shown to elicit innate immunity through the TLR2/MyD88-dependent pathway and TLR-

independent production of IFN-β (40), the ability of the virus to provide persistent TLR signals for immunotherapy in a setting of established tolerance together with the CXCR4 antagonist-mediated reduction in intratumoral immunosuppressive elements may produce a more permissive environment for antitumor immunity.

The induction of anti-WT1 antibody and $CD8^+$ T cell responses during the oncolytic virotherapy treatment holds important implications for immunotherapy because WT1 is one of the immunogenic tumor antigens expressed at high levels in a variety of human neoplasms including EOC (69, 70). *WT1* encodes a zinc-finger protein which plays a crucial role in the normal development of several organs (71), and is essential for repression of the epithelial phenotype in epicardial cells and during embryonic stem cell differentiation through direct transcriptional regulation of genes encoding Snail and E-cadherin (72). Because both genes are mediators of epithelial-mesenchymal transition (72), which is a key developmental program that is often activated during cancer invasion and development of CICs (18, 73), expression of WT1 in spheres isolated from ID8-T cells (data not shown) suggests that it may serve as a target for T cell-mediated activity. Previous studies have demonstrated that DCs pulsed with the lysates of CIC-enriched populations from histologically distinct murine tumors conferred antitumor immunity which was associated with the induction of humoral and cellular responses that directly targeted CICs via complement-dependent cytotoxicity and CTLs, respectively (74). In our studies, WT1-specific antibodies could not have been directly involved in tumor cell lysis because WT1 is expressed intracellularly. However, the antibodies could form immune complexes with WT1 protein released from lysed tumor cells and facilitate enhanced antigen presentation to Fc receptors on DCs (75). On the other hand, the lysis of tumor cells by CTLs may extend the remission period or even lead to tumor-free survival, particularly if some of these activities are directed against CICs. Consistent with this notion, ~10% lysis at the 100:1 effector-to-target ratio was detected in cultures of spheroid cells incubated overnight with IFN-γ for stimulation of MHC class I expression before the CTL assay (not shown), stressing the need for additional studies to facilitate a more effective killing of these cells. Altogether, the presented mechanism of inhibition of pathways promoting tumor growth is likely applicable to different cancer types and can potentially unravel novel therapeutic avenues that efficiently target CICs to minimize the risk of tumor recurrence in cancer patients.

Supplementary Material

Refer to Web version on PubMed Central for supplementary material.

Acknowledgments

We are grateful to Dr. M. Clarke for reagents.

Abbreviations used in this paper

ALDH1	aldehyde dehydrogenase isoform 1
BM	bone marrow

CICs	cancer initiating cells
DCs	dendritic cells
EGFP	enhanced green fluorescence protein
EOC	epithelial ovarian carcinoma
EPCs	endothelial progenitor cells
OVV	oncolytic vaccinia virus
TILs	tumor-infiltrating lymphocytes
Tregs	regulatory T-cells
VEGF	vascular endothelial growth factor
WT1	Wilms' tumor antigen 1

References

1. Jemal A, Siegel R, Ward E, Murray T, Xu J, Thun MJ. Cancer statistics. CA Cancer J Clin. 2007; 57:43–66. [PubMed: 17237035]
2. Kajiyama H, Shibata K, Terauchi M, Ino K, Nawa A, Kikkawa F. Involvement of SDF-1alpha/CXCR4 axis in the enhanced peritoneal metastasis of epithelial ovarian carcinoma. Int J Cancer. 2008; 122:91–99. [PubMed: 17893878]
3. Sorensen EW, Gerber SA, Sedlacek AL, Rybalko VY, Chan WM, Lord EM. Omental immune aggregates and tumor metastasis within the peritoneal cavity. Immunol Res. 2009; 45:185–194. [PubMed: 19253004]
4. Armstrong D. Update on treatment options for newly diagnosed ovarian cancer. Clin Adv Hematol Oncol. 2010; 8:675–678. [PubMed: 21317863]
5. Shah MM, Landen CN. Ovarian cancer stem cells: Are they real and why are they important? Gynecol Oncol. 201310.1016/j.ygyno.2013.12.001
6. Foster R, Buckanovich RJ, Rueda BR. Ovarian cancer stem cells: working towards the root of stemness. Cancer Lett. 2013; 338:147–157. [PubMed: 23138176]
7. Bapat SA, Mali AM, Koppikar CB, Kurrey NK. Stem and progenitor-like cells contribute to the aggressive behavior of human epithelial ovarian cancer. Cancer Res. 2005; 65:3025–3029. [PubMed: 15833827]
8. Kryczek I, Liu S, Roh M, Vatan L, Szeliga W, Wei S, Banerjee M, Mao Y, Kotarski J, Wicha MS, Liu R, Zou W. Expression of aldehyde dehydrogenase and Cd133 defines ovarian cancer stem cells. Int J Cancer. 2011; 130:29–39. [PubMed: 21480217]
9. Steffensen KD, Alvero AB, Yang Y, Waldstrom M, Hui P, Holmberg JC, Silasi DA, Jakobsen A, Rutherford T, Mor G. Prevalence of epithelial ovarian cancer stem cells correlates with recurrence in early-stage ovarian cancer. J Oncol. 2011; 2011:620523. [PubMed: 21904548]
10. Zhan Q, Wang C, Ngai S. Ovarian cancer stem cells: a new target for cancer therapy. Biomed Res Int. 2013; 2013:916819. [PubMed: 23509802]
11. Zhang S, Balch C, Chan MW, Lai HC, Matei D, Schilder JM, Yan PS, Huang TH, Nephew KP. Identification and characterization of ovarian cancer-initiating cells from primary human tumors. Cancer Res. 2008; 68:4311–4320. [PubMed: 18519691]
12. Liao J, Qian F, Tchabo NN, Mhawech-Fauceglia P, Beck A, Qian Z, Wang X, Huss WJ, Lele SB, Morrison CD, Odunsi K. Ovarian Cancer Spheroid Cells with Stem Cell-Like Properties Contribute to Tumor Generation, Metastasis and Chemotherapy Resistance through Hypoxia-Resistant Metabolism. PLoS One. 2014; 9:e84941. [PubMed: 24409314]

13. Sato E, Olson SH, Ahn J, Bundy B, Nishikawa H, Qian F, Jungbluth AA, Frosina D, Gnjatic S, Ambrosone C, Kepner J, Odunsi T, Ritter G, Lele S, Chen YT, Ohtani H, Old LJ, Odunsi K. Intraepithelial CD8+ tumor-infiltrating lymphocytes and a high CD8+/regulatory T cell ratio are associated with favorable prognosis in ovarian cancer. Proc Natl Acad Sci USA. 2005; 102:18538–18543. [PubMed: 16344461]
14. Odunsi K, Qian F, Matsuzaki J, Mhawech-Fauceglia P, Andrews C, Hoffman EW, Pan L, Ritter G, Villella J, Thomas B, Rodabaugh K, Lele S, Shrikant P, Old LJ, Gnjatic S. Vaccination with an NY-ESO-1 peptide of HLA class I/II specificities induces integrated humoral and T cell responses in ovarian cancer. Proc Natl Acad Sci USA. 2007; 104:12837–12842. [PubMed: 17652518]
15. Hwang WT, Adams SF, Tahirovic E, Hagemann IS, Coukos G. Prognostic significance of tumor-infiltrating T cells in ovarian cancer: a meta-analysis. Gynecol Oncol. 2012; 124:192–198. [PubMed: 22040834]
16. Cojoc M, Peitzsch C, Trautmann F, Polishchuk L, Telegeev GD, Dubrovska A. Emerging targets in cancer management: role of the CXCL12/CXCR4 axis. Onco Targets Ther. 2013; 6:1347–1361. [PubMed: 24124379]
17. Gelmini S, Mangoni M, Serio M, Romagnani P, Lazzeri E. The critical role of SDF-1/CXCR4 axis in cancer and cancer stem cells metastasis. J Endocrinol Invest. 2008; 31:809–819. [PubMed: 18997494]
18. Visvader JE, Lindeman GJ. Cancer stem cells in solid tumours: accumulating evidence and unresolved questions. Nat Rev Cancer. 2008; 8:755–768. [PubMed: 18784658]
19. Kucia M, Reca R, Miekus K, Wanzeck J, Wojakowski W, Janowska-Wieczorek A, Ratajczak J, Ratajczak MZ. Trafficking of normal stem cells and metastasis of cancer stem cells involve similar mechanisms: pivotal role of the SDF-1-CXCR4 axis. Stem Cells. 2005; 23:879–894. [PubMed: 15888687]
20. Scotton CJ, Wilson JL, Scott K, Stamp G, Wilbanks GD, Fricker S, Bridger G, Balkwill FR. Multiple actions of the chemokine CXCL12 on epithelial tumor cells in human ovarian cancer. Cancer Res. 2002; 62:5930–5938. [PubMed: 12384559]
21. Kryczek I, Lange A, Mottram P, Alvarez X, Cheng P, Hogan M, Moons L, Wei S, Zou L, Machelon VV, Emilie D, Terrassa M, Lackner A, Curiel TJ, Carmeliet P, Zou W. CXCL12 and vascular endothelial growth factor synergistically induce neoangiogenesis in human ovarian cancers. Cancer Res. 2005; 65:465–472. [PubMed: 15695388]
22. Kryczek I, Wei S, Keller E, Liu R, Zou W. Stroma-derived factor (SDF-1/CXCL12) and human tumor pathogenesis. Am J Physiol Cell Physiol. 2007; 292:C987–995. [PubMed: 16943240]
23. Orimo A, Gupta PB, Sgroi DC, Arenzana-Seisdedos F, Delaunay T, Naeem R, Carey VJ, Richardson AL, Weinberg RA. Stromal fibroblasts present in invasive human breast carcinomas promote tumor growth and angiogenesis through elevated SDF-1/CXCL12 secretion. Cell. 2005; 121:335–348. [PubMed: 15882617]
24. Obermajer N, Muthuswamy R, Odunsi K, Edwards RP, Kalinski P. PGE(2)-induced CXCL12 production and CXCR4 expression controls the accumulation of human MDSCs in ovarian cancer environment. Cancer Res. 2011; 71:7463–7470. [PubMed: 22025564]
25. Zou W, Machelon V, Coulomb-L'Hermin A, Borvak J, Nome F, Isaeva T, Wei S, Krzysiek R, Durand-Gasselin I, Gordon A, Pustilnik T, Curiel DT, Galanaud P, Capron F, Emilie D, Curiel TJ. Stromal-derived factor-1 in human tumors recruits and alters the function of plasmacytoid precursor dendritic cells. Nat Med. 2001; 7:1339–1346. [PubMed: 11726975]
26. Righi E, Kashiwagi S, Yuan J, Santosuosso M, Leblanc P, Ingraham R, Forbes B, Edelblute B, Collette B, Xing D, Kowalski M, Mingari MC, Vianello F, Birrer M, Orsulic S, Dranoff G, Poznansky MC. CXCL12/CXCR4 blockade induces multimodal antitumor effects that prolong survival in an immunocompetent mouse model of ovarian cancer. Cancer Res. 71:5522–5534. [PubMed: 21742774]
27. Curiel TJ, Coukos G, Zou L, Alvarez X, Cheng P, Mottram P, Evdemon-Hogan M, Conejo-Garcia JR, Zhang L, Burow M, Zhu Y, Wei S, Kryczek I, Daniel B, Gordon A, Myers L, Lackner A, Disis ML, Knutson KL, Chen L, Zou W. Specific recruitment of regulatory T cells in ovarian carcinoma fosters immune privilege and predicts reduced survival. Nat Med. 2004; 10:942–949. [PubMed: 15322536]

28. Devine SM, Flomenberg N, Vesole DH, Liesveld J, Weisdorf D, Badel K, Calandra G, DiPersio JF. Rapid mobilization of CD34+ cells following administration of the CXCR4 antagonist AMD3100 to patients with multiple myeloma and non-Hodgkin's lymphoma. J Clin Oncol. 2004; 22:1095–1102. [PubMed: 15020611]
29. Wong D, Korz W. Translating an Antagonist of Chemokine Receptor CXCR4: from bench to bedside. Clin Cancer Res. 2008; 14:7975–7980. [PubMed: 19088012]
30. Hassan S, Buchanan M, Jahan K, Aguilar-Mahecha A, Gaboury L, Muller WJ, Alsawafi Y, Mourskaia AA, Siegel PM, Salvucci O, Basik M. CXCR4 peptide antagonist inhibits primary breast tumor growth, metastasis and enhances the efficacy of anti-VEGF treatment or docetaxel in a transgenic mouse model. Int J Cancer. 2011; 129:225–232. [PubMed: 20830712]
31. Huang EH, Singh B, Cristofanilli M, Gelovani J, Wei C, Vincent L, Cook KR, Lucci A. A CXCR4 antagonist CTCE-9908 inhibits primary tumor growth and metastasis of breast cancer. J Surg Res. 2009; 155:231–236. [PubMed: 19482312]
32. Gupta SK, Pillarisetti K. Cutting edge: CXCR4-Lo: molecular cloning and functional expression of a novel human CXCR4 splice variant. J Immunol. 1999; 163:2368–2372. [PubMed: 10452968]
33. Burger JA, Kipps TJ. CXCR4: a key receptor in the crosstalk between tumor cells and their microenvironment. Blood. 2006; 107:1761–1767. [PubMed: 16269611]
34. Broxmeyer HE, Orschell CM, Clapp DW, Hangoc G, Cooper S, Plett PA, Liles WC, Li X, Graham-Evans B, Campbell TB, Calandra G, Bridger G, Dale DC, Srour EF. Rapid mobilization of murine and human hematopoietic stem and progenitor cells with AMD3100, a CXCR4 antagonist. J Exp Med. 2005; 201:1307–1318. [PubMed: 15837815]
35. Gil M, Seshadri M, Komorowski MP, Abrams SI, Kozbor D. Targeting CXCL12/CXCR4 signaling with oncolytic virotherapy disrupts tumor vasculature and inhibits breast cancer metastases. Proc Natl Acad Sci USA. 2013; 110:E1291–1300. [PubMed: 23509246]
36. Kirn DH, Thorne SH. Targeted and armed oncolytic poxviruses: a novel multi-mechanistic therapeutic class for cancer. Nat Rev Cancer. 2009; 9:64–71. [PubMed: 19104515]
37. Parato KA, Breitbach CJ, Le Boeuf F, Wang J, Storbeck C, Ilkow C, Diallo JS, Falls T, Burns J, Garcia V, Kanji F, Evgin L, Hu K, Paradis F, Knowles S, Hwang TH, Vanderhyden BC, Auer R, Kirn DH, Bell JC. The oncolytic poxvirus JX-594 selectively replicates in and destroys cancer cells driven by genetic pathways commonly activated in cancers. Mol Ther. 2012; 20:749–758. [PubMed: 22186794]
38. Vanderplasschen A, Mathew E, Hollinshead M, Sim RB, Smith GL. Extracellular enveloped vaccinia virus is resistant to complement because of incorporation of host complement control proteins into its envelope. Proc Natl Acad Sci U S A. 1998; 95:7544–7549. [PubMed: 9636186]
39. Yang Y, Huang CT, Huang X, Pardoll DM. Persistent Toll-like receptor signals are required for reversal of regulatory T cell-mediated CD8 tolerance. Nat Immunol. 2004; 5:508–515. [PubMed: 15064759]
40. Zhu J, Martinez J, Huang X, Yang Y. Innate immunity against vaccinia virus is mediated by TLR2 and requires TLR-independent production of IFN-beta. Blood. 2007; 109:619–625. [PubMed: 16973959]
41. Wang H, Chen NG, Minev BR, Szalay AA. Oncolytic vaccinia virus GLV-1h68 strain shows enhanced replication in human breast cancer stem-like cells in comparison to breast cancer cells. J Transl Med. 2012; 10:167. [PubMed: 22901246]
42. Janat-Amsbury MM, Yockman JW, Anderson ML, Kieback DG, Kim SW. Comparison of ID8 MOSE and VEGF-modified ID8 cell lines in an immunocompetent animal model for human ovarian cancer. Anticancer Res. 2006; 26:2785–2789. [PubMed: 16886597]
43. Goncharenko-Khaider N, Lane D, Matte I, Rancourt C, Piche A. The inhibition of Bid expression by Akt leads to resistance to TRAIL-induced apoptosis in ovarian cancer cells. Oncogene. 2010; 29:5523–5536. [PubMed: 20661217]
44. Schneider-Gadicke A, Schwarz E. Different human cervical carcinoma cell lines show similar transcription patterns of human papillomavirus type 18 early genes. EMBO J. 1986; 5:2285–2292. [PubMed: 3023067]
45. Jensen FC, Girardi AJ, Gilden RV, Koprowski H. Infection of Human and Simian Tissue Cultures with Rous Sarcoma Virus. Proc Natl Acad Sci USA. 1964; 52:53–59. [PubMed: 14192657]

46. Chakrabarti S, Sisler JR, Moss B. Compact, synthetic, vaccinia virus early/late promoter for protein expression. Biotechniques. 1997; 23:1094–1097. [PubMed: 9421642]
47. Gil M, Bieniasz M, Seshadri M, Fisher D, Ciesielski MJ, Chen Y, Pandey RK, Kozbor D. Photodynamic therapy augments the efficacy of oncolytic vaccinia virus against primary and metastatic tumours in mice. Br J Cancer. 2011; 105:1512–1521. [PubMed: 21989183]
48. Gil M, Bieniasz M, Wierzbicki A, Bambach BJ, Rokita H, Kozbor D. Targeting a mimotope vaccine to activating Fcgamma receptors empowers dendritic cells to prime specific CD8+ T cell responses in tumor-bearing mice. J Immunol. 2009; 183:6808–6818. [PubMed: 19846865]
49. Liang Z, Brooks J, Willard M, Liang K, Yoon Y, Kang S, Shim H. CXCR4/CXCL12 axis promotes VEGF-mediated tumor angiogenesis through Akt signaling pathway. Biochem Biophys Res Commun. 2007; 359:716–722. [PubMed: 17559806]
50. Ferrara N. Vascular endothelial growth factor as a target for anticancer therapy. Oncologist. 2004; 9(Suppl 1):2–10. [PubMed: 15178810]
51. Ferrara N. Vascular endothelial growth factor: basic science and clinical progress. Endocr Rev. 2004; 25:581–611. [PubMed: 15294883]
52. Shen GH, Ghazizadeh M, Kawanami O, Shimizu H, Jin E, Araki T, Sugisaki Y. Prognostic significance of vascular endothelial growth factor expression in human ovarian carcinoma. Br J Cancer. 2000; 83:196–203. [PubMed: 10901370]
53. Liu BY, Soloviev L, Chang P, Lee J, Huang X, Zhong C, Ferrara N, Polakis P, Sakanaka C. Stromal cell-derived factor-1/CXCL12 contributes to MMTV-Wnt1 tumor growth involving Gr1+CD11b+ cells. PLoS One. 2010; 5:e8611. [PubMed: 20087418]
54. Orimo A, Weinberg RA. Stromal fibroblasts in cancer: a novel tumor-promoting cell type. Cell Cycle. 2006; 5:1597–1601. [PubMed: 16880743]
55. Nozawa H, Chiu C, Hanahan D. Infiltrating neutrophils mediate the initial angiogenic switch in a mouse model of multistage carcinogenesis. Proc Natl Acad Sci U S A. 2006; 103:12493–12498. [PubMed: 16891410]
56. Curiel TJ, Cheng P, Mottram P, Alvarez X, Moons L, Evdemon-Hogan M, Wei S, Zou L, Kryczek I, Hoyle G, Lackner A, Carmeliet P, Zou W. Dendritic cell subsets differentially regulate angiogenesis in human ovarian cancer. Cancer Res. 2004; 64:5535–5538. [PubMed: 15313886]
57. Nathan C. Neutrophils and immunity: challenges and opportunities. Nat Rev Immunol. 2006; 6:173–182. [PubMed: 16498448]
58. Youn JI, Collazo M, Shalova IN, Biswas SK, Gabrilovich DI. Characterization of the nature of granulocytic myeloid-derived suppressor cells in tumor-bearing mice. J Leukoc Biol. 2012; 91:167–181. [PubMed: 21954284]
59. Breitbach CJ, Paterson JM, Lemay CG, Falls TJ, McGuire A, Parato KA, Stojdl DF, Daneshmand M, Speth K, Kirn D, McCart JA, Atkins H, Bell JC. Targeted inflammation during oncolytic virus therapy severely compromises tumor blood flow. Mol Ther. 2007; 15:1686–1693. [PubMed: 17579581]
60. Wei S, Kryczek I, Zou L, Daniel B, Cheng P, Mottram P, Curiel T, Lange A, Zou W. Plasmacytoid dendritic cells induce CD8+ regulatory T cells in human ovarian carcinoma. Cancer Res. 2005; 65:5020–5026. [PubMed: 15958543]
61. Singh P, Yao Y, Weliver A, Broxmeyer HE, Hong SC, Chang CH. Vaccinia virus infection modulates the hematopoietic cell compartments in the bone marrow. Stem Cells. 2008; 26:1009–1016. [PubMed: 18258722]
62. Acharyya S, Oskarsson T, Vanharanta S, Malladi S, Kim J, Morris PG, Manova-Todorova K, Leversha M, Hogg N, Seshan VE, Norton L, Brogi E, Massague J. A CXCL1 paracrine network links cancer chemoresistance and metastasis. Cell. 2012; 150:165–178. [PubMed: 22770218]
63. Shepherd TG, Theriault BL, Campbell EJ, Nachtigal MW. Primary culture of ovarian surface epithelial cells and ascites-derived ovarian cancer cells from patients. Nat Protoc. 2006; 1:2643–2649. [PubMed: 17406520]
64. Naito T, Kaneko Y, Kozbor D. Oral vaccination with modified vaccinia virus Ankara attached covalently to TMPEG-modified cationic liposomes overcomes pre-existing poxvirus immunity from recombinant vaccinia immunization. J Gen Virol. 2007; 88:61–70. [PubMed: 17170437]

65. Kusumbe AP, Bapat SA. Cancer stem cells and aneuploid populations within developing tumors are the major determinants of tumor dormancy. Cancer Res. 2009; 69:9245–9253. [PubMed: 19951996]
66. Kleffel S, Schatton T. Tumor dormancy and cancer stem cells: two sides of the same coin? Adv Exp Med Biol. 2013; 734:145–179. [PubMed: 23143979]
67. Aguirre-Ghiso JA. Models, mechanisms and clinical evidence for cancer dormancy. Nat Rev Cancer. 2007; 7:834–846. [PubMed: 17957189]
68. Russell SJ, Peng KW, Bell JC. Oncolytic virotherapy. Nat Biotechnol. 2012; 30:658–670. [PubMed: 22781695]
69. Inoue K, Sugiyama H, Ogawa H, Nakagawa M, Yamagami T, Miwa H, Kita K, Hiraoka A, Masaoka T, Nasu K, Kyo T, Dohy H, Nakauchi H, Ishidate T, Akiyama T, Kishimoto T. WT1 as a new prognostic factor and a new marker for the detection of minimal residual disease in acute leukemia. Blood. 1994; 84:3071–3079. [PubMed: 7949179]
70. Hylander B, Repasky E, Shrikant P, Intengan M, Beck A, Driscoll D, Singhal P, Lele S, Odunsi K. Expression of Wilms tumor gene (WT1) in epithelial ovarian cancer. Gynecol Oncol. 2006; 101:12–17. [PubMed: 16263157]
71. Hohenstein P, Hastie ND. The many facets of the Wilms' tumour gene, WT1. Hum Mol Genet. 2006; 15:R196–201. [PubMed: 16987884]
72. Martinez-Estrada OM, Lettice LA, Essafi A, Guadix JA, Slight J, Velecela V, Hall E, Reichmann J, Devenney PS, Hohenstein P, Hosen N, Hill RE, Munoz-Chapuli R, Hastie ND. Wt1 is required for cardiovascular progenitor cell formation through transcriptional control of Snail and E-cadherin. Nat Genet. 2010; 42:89–93. [PubMed: 20023660]
73. Mani SA, Guo W, Liao MJ, Eaton EN, Ayyanan A, Zhou AY, Brooks M, Reinhard F, Zhang CC, Shipitsin M, Campbell LL, Polyak K, Brisken C, Yang J, Weinberg RA. The epithelial-mesenchymal transition generates cells with properties of stem cells. Cell. 2008; 133:704–715. [PubMed: 18485877]
74. Ning N, Pan Q, Zheng F, Teitz-Tennenbaum S, Egenti M, Yet J, Li M, Ginestier C, Wicha MS, Moyer JS, Prince ME, Xu Y, Zhang XL, Huang S, Chang AE, Li Q. Cancer stem cell vaccination confers significant antitumor immunity. Cancer Res. 2012; 72:1853–1864. [PubMed: 22473314]
75. Dhodapkar MV, Steinman RM, Sapp M, Desai H, Fossella C, Krasovsky J, Donahoe SM, Dunbar PR, Cerundolo V, Nixon DF, Bharadwaj N. Rapid generation of broad T-cell immunity in humans after a single injection of mature dendritic cells. J Clin Invest. 1999; 104:173–180. [PubMed: 10411546]

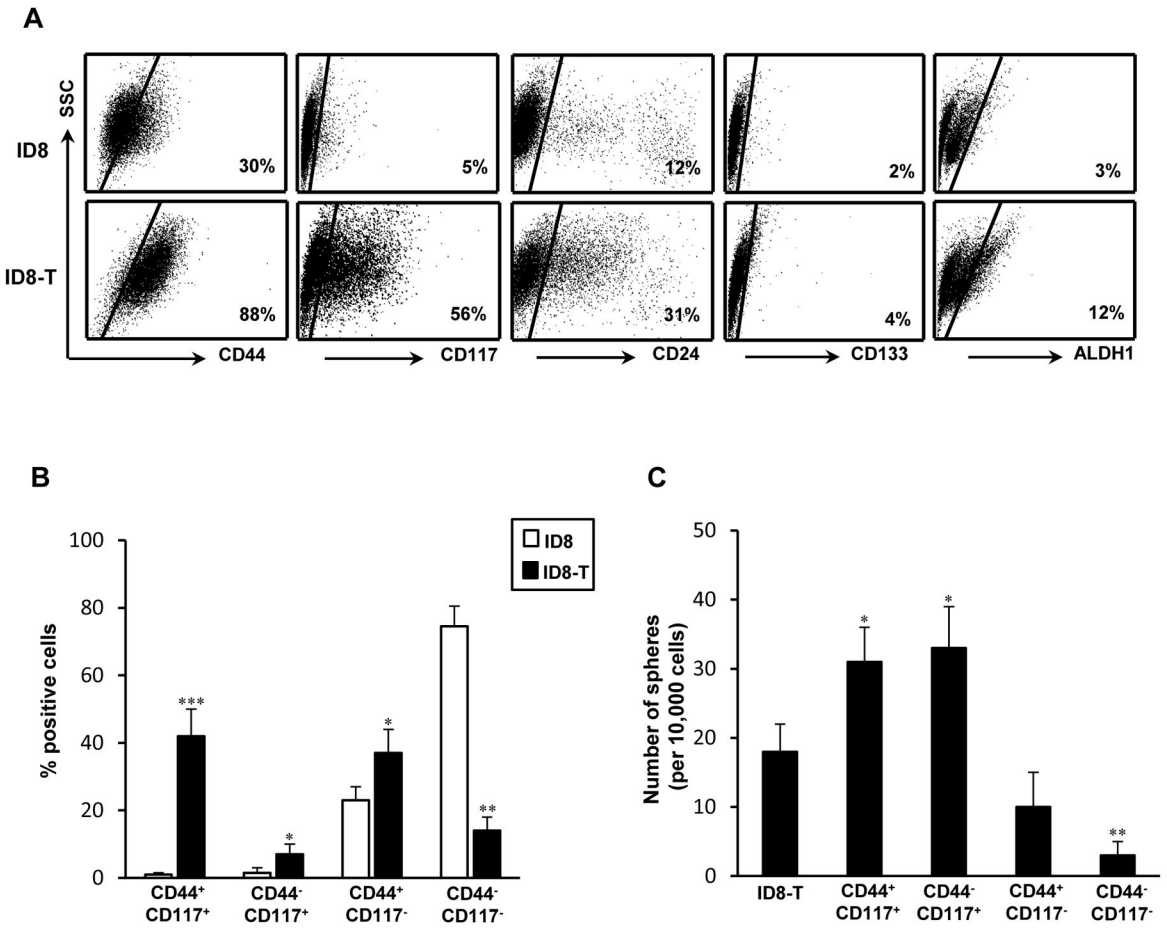

FIGURE 1.

Phenotypic characterization and sphere-forming ability of ID8-T ovarian tumor cells and their subsets positive or negative for CD44 and CD117 antigen expression. (**A**) Flow cytometry analysis of CD117, CD44, CD24, and CD133 expression in parental ID8 and ID8-T variant was performed on single-cell suspensions with marker-specific mAbs. Background staining was assessed using an isotype control Abs. The ALDEFLUOR (ALDH1) kit was used to identify $ALDH1^+$ cells with high ALDH1 enzymatic activity. In each experiment, the specific ALDH inhibitor diethylaminobenzaldehyde was used as a negative control. Data are from one representative experiment of three performed. (**B**) ID8 and ID8-T tumor cells were analyzed by flow cytometry for expression of CD44 and CD117 antigens. Percentages of $CD117^+CD44^+$, $CD117^+CD44^-$, $CD117^-CD44^+$, and $CD117^-CD44^-$ were presented as the mean ± SD of three experiments. (**C**) The sphere-forming assay was performed with ID8-T cell line and its sorted subsets positive or negative for CD44 and CD117 antigen expression. Numbers of spheres were expressed as means ± SD. $*P < 0.05$, $**P < 0.01$, and $***P < 0.001$.

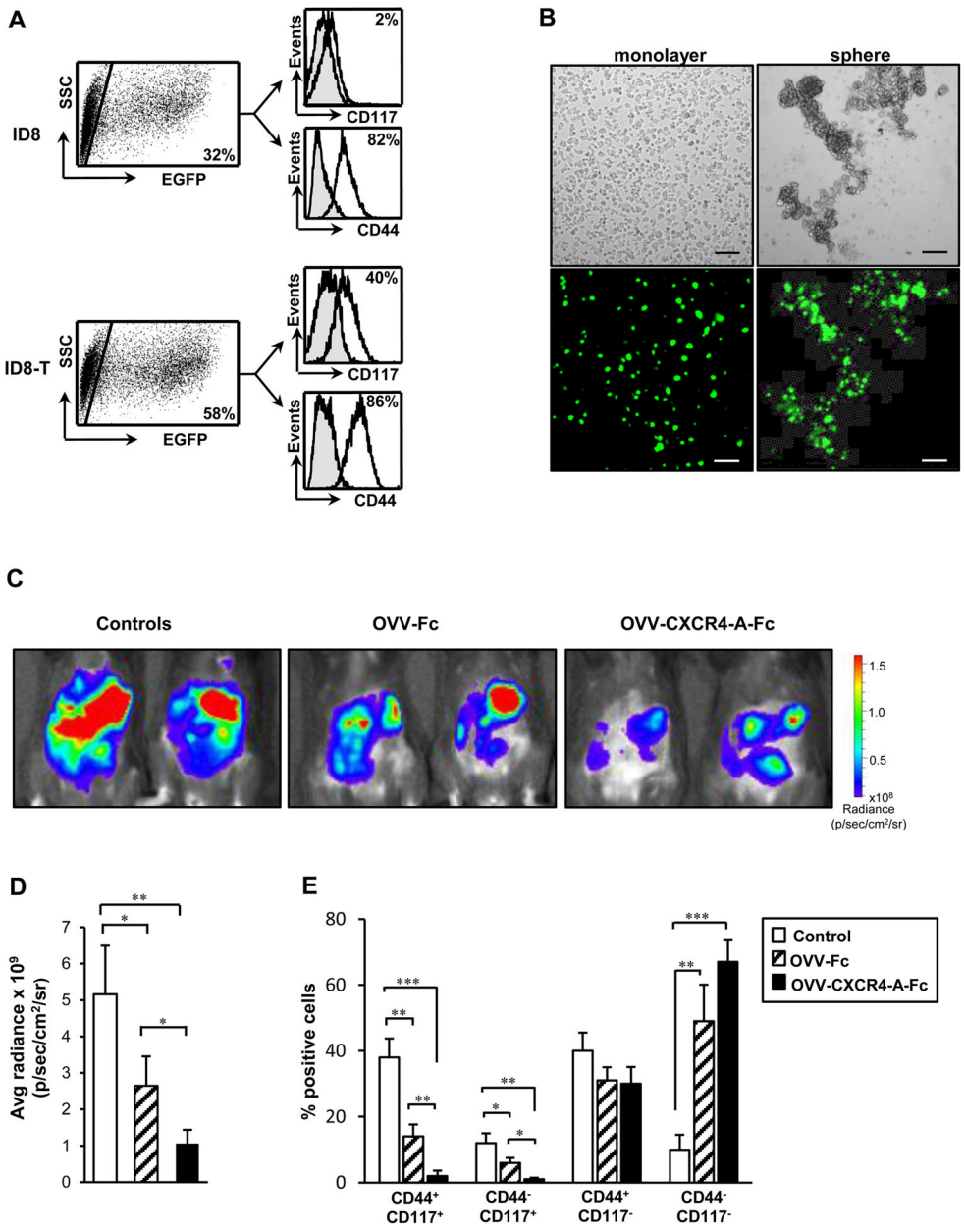

FIGURE 2.

Susceptibility of ID8-T tumor cells to vaccinia virus infection. (**A**) ID8 and ID8-T cells were infected with OVV-EGFP (MOI = 1) and analyzed by flow cytometry 12 h later to determine expression of EGFP in $CD44^+$ and $CD117^+$ tumor cells (*right panel*). (**B**) ID8-T cells were cultured as a monolayer or in serum-free condition medium for 12 days before infection with OVV-EGFP (MOI = 1). The expression of EGFP in infected cells was examined under immunofluorescence microscope 12 h later. Scale bars, 25 μm. (**C**) ID8-T cells (5×10^5 cells) were injected i.p. to syngeneic C57BL/6 mice and treated with OVV-Fc or OVV-CXCR4-A-Fc (10^8 PFU) after 7 days. The viruses were delivered i.p. and the effect of the treatments on tumor growth was determined by bioluminescence imaging 8 days later.

(**D**) Quantification of the bioluminescent signals from the tumor regions is depicted. Error bars represent the SD of the mean of three experiments with 3 – 4 mice per group. (**E**) ID8-T tumor cells were isolated from peritoneal cavities 8 days after the treatment and analyzed by flow cytometry for expression of CD117 and CD44 antigens. Percentages of $CD117^{+}CD44^{+}$, $CD117^{+}CD44^{-}$, $CD117^{-}CD44^{+}$, and $CD117^{-}CD44^{-}$ were presented as the means ± SD. $^{*}P < 0.05$, $^{**}P < 0.01$, and $^{***}P < 0.001$.

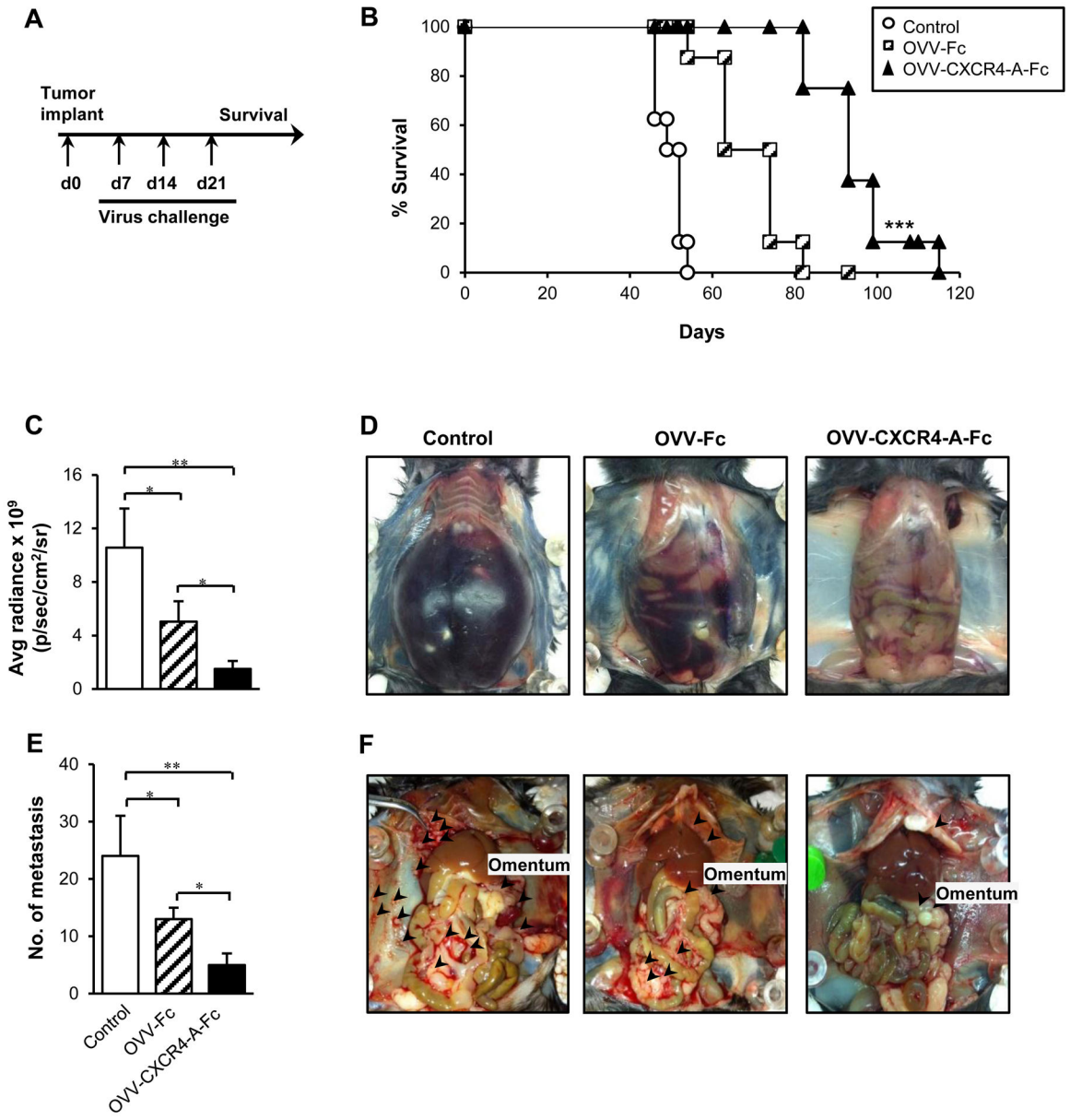

FIGURE 3.

Effect of OVV-CXCR4-A-Fc on orthotopic ID8-T tumor growth. (**A**) ID8-T-bearing C57BL/6 mice were treated with OVV-Fc or OVV-CXCR4-A-Fc on days 7, 14 and 21 after i.p. tumor challenge and monitored for survival. Control mice were treated with PBS. (**B**) Survival was defined as the point at which mice were killed because of extensive tumor burden (i.e., experimental/humane endpoints). Kaplan-Meier survival plots were prepared and significance was determined using the log-rank method. (**C**) ID8-T tumor growth was quantified at the time of development of bloody ascites (**D**) in control mice. (**E**) Metastatic dissemination in the omentum, diaphragm, mesentery and peritoneal wall was assessed by counting metastatic colonies (> 5 mm) in individual mice and presented as the means ± SD of three mice. (**F**) ID8-T-bearing mice with abdominal swelling were sacrificed and organs

were examined for tumor development and metastatic spread. Representative images of metastasis within peritoneal cavities in control, OVV-Fc- and OVV-CXCR4-A-Fc-treated mice are shown. ***$P < 0.001$ vs. OVV-Fc-treated mice.

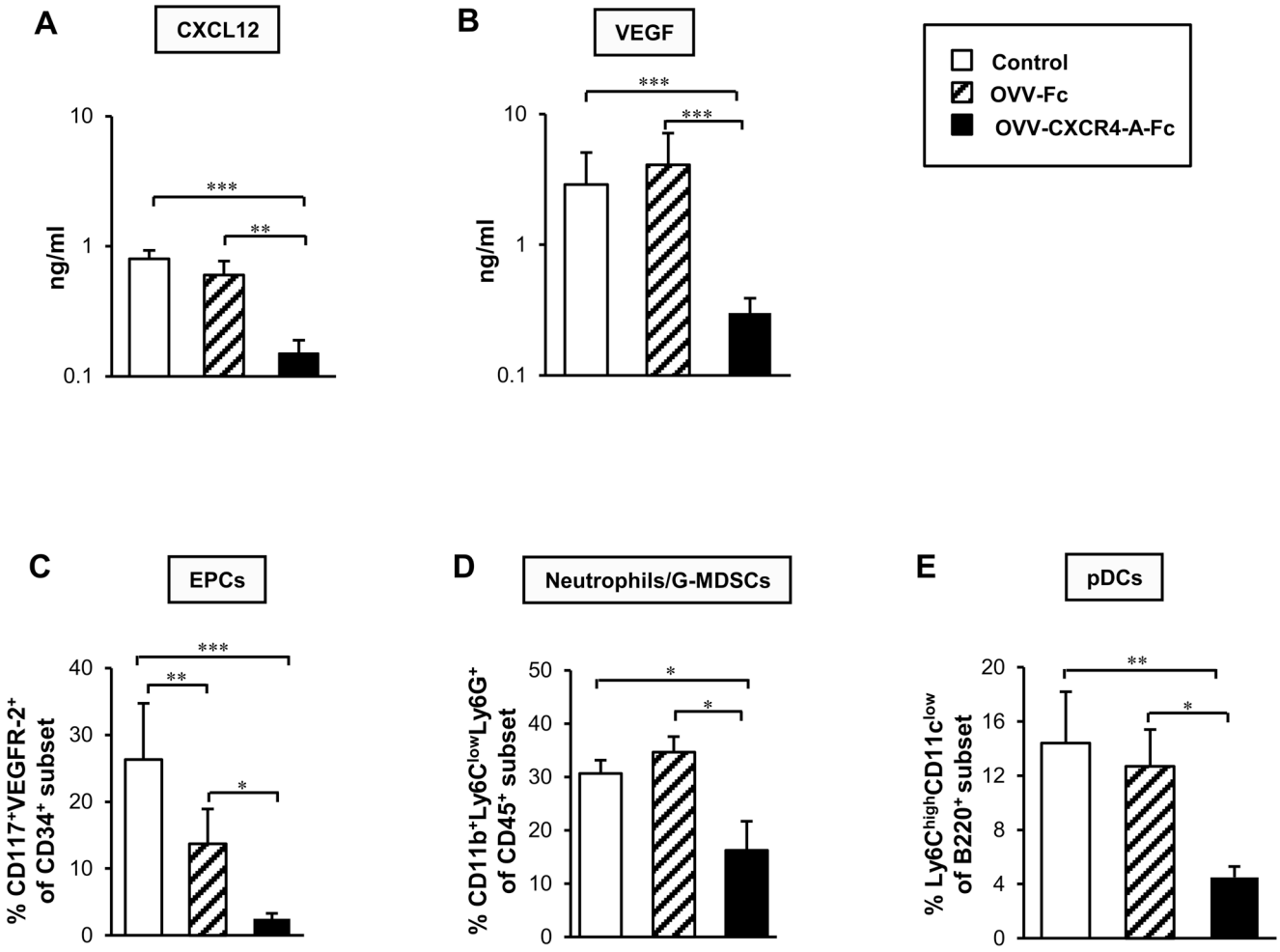

FIGURE 4.

Assessment of OVV-CXCR4-A-Fc-induced changes in the tumor microenvironment. (**A** and **B**) Expression levels of CXCL12 and VEGF in peritoneal fluids harvested from tumor-bearing mice at the time the control mice developed abdominal swelling, which roughly corresponded to 40 days after tumor challenge, were determined by ELISA. (**C**) Recruitments of EPCs ($CD34^+$ $CD117^+VEGFR2^+$), (**D**) neutrophils/G-MDSCs ($CD11b^+Ly6C^{low}$ $Ly6G^+$), and (**E**) pDCs ($B220^{high}Ly6C^{high}$ $CD11c^{low}$) into ascites-derived ID8-T tumor in control and virally-treated mice were analyzed by flow cytometry as described in *Material and Methods* section. Background staining was assessed using isotype control antibodies. Results are presented as the means ± SD of three or four independent experiments. *$P < 0.05$, **$P < 0.01$, ***$P < 0.001$.

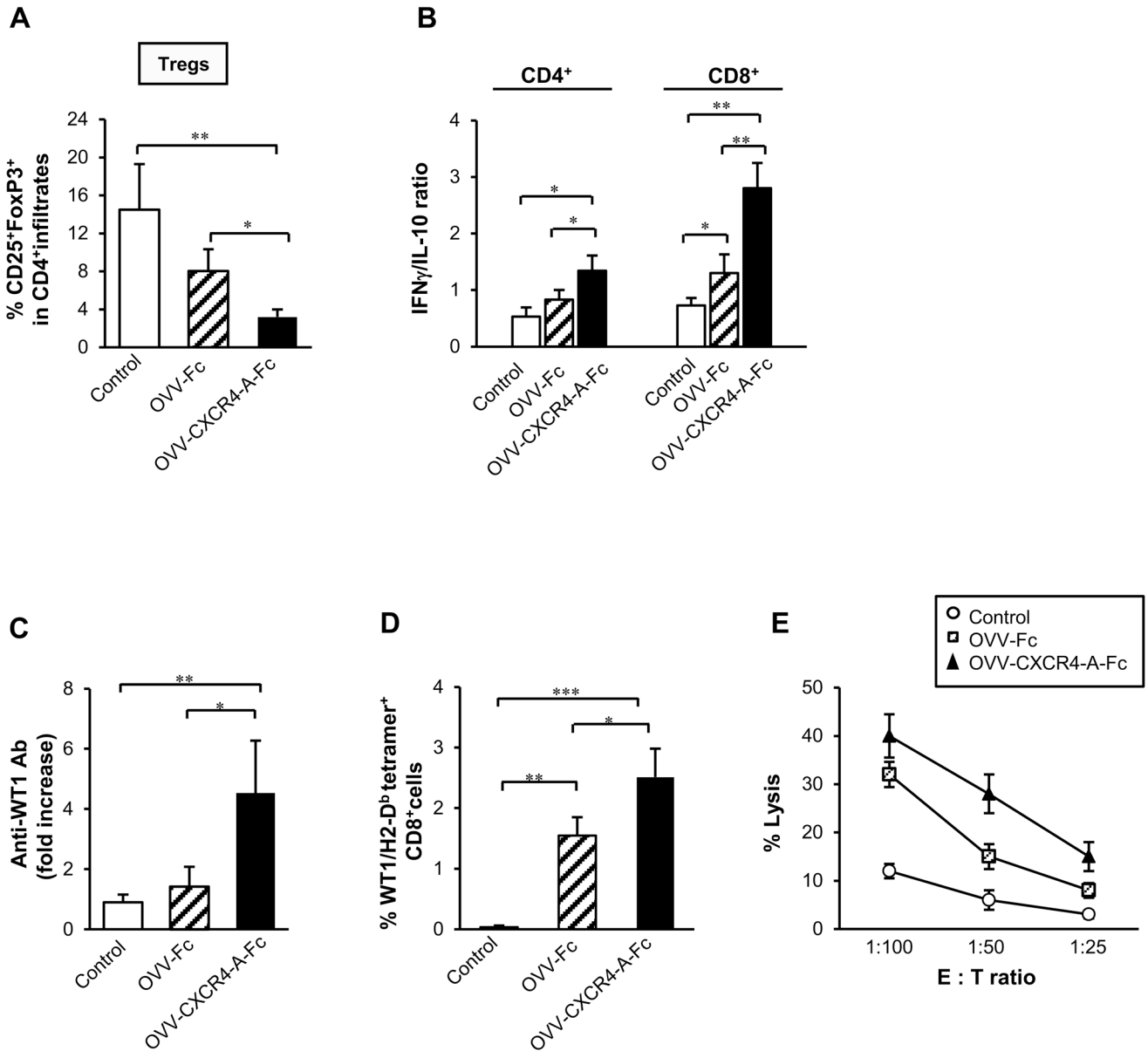

FIGURE 5.

OVV-CXCR4-A-Fc inhibits tumor immunosuppressive networks and promotes induction of antitumor immune responses. (**A**) The numbers of Tregs in ascites-derived tumors of control and virally-treated mice were analyzed by flow cytometry after staining of single-cell suspensions with anti-CD45-APC, anti-CD4-PE, anti-CD25-FITC and anti-FoxP3-AlexaFluor 647. (**B**) The ratios of IFN-γ/IL-10-expressing $CD4^+$ and $CD8^+$ TILs were determined by intracellular staining with rat mAbs against mouse IFN-γ-PE or IL-10-PE followed CD4-PECy5 or CD8-PECy5 followed by flow cytometry. Background staining was assessed using isotype control antibodies. Results are presented as the means ± SD of three or four independent experiments. (**C**) Sera were collected from tumor-bearing mice before viral challenge and at the time the control mice developed ascites and analyzed by ELISA for the presence of antibodies to WT1 antigen. All samples were analyzed in

triplicates with serum dilution of 1:100. (**D**) The percent of $WT1_{126-134}$ tetramer-specific $CD8^+$ T cells was determined in lymphocytes obtained from axillary, brachial and inguinal lymph nodes isolated from the same group of animals that were analyzed for humoral responses. The isolated cells were incubated with LPS-matured $WT1_{126-134}$ peptide-coated DCs for 72 h in the presence of IL-2, washed and stained with anti-CD8-PECy5 mAb and PE-labeled H-$2D^b$-restricted $WT1_{126-134}$ tetramer. All evaluations were performed on FACScalibur flow cytometer. After gating on forward and side scatter parameters, at least 10,000 gated events were routinely acquired and analyzed using CellQuest software. (**E**) ID8-T -specific CTL responses. $CD8^+$ splenocytes from untreated, OVV-Fc- and OVV-CXCR4-A-Fc-treated tumor-bearing mice were cultured with $WT1_{126-134}$ peptide-coated DCs at the 20:1 ratio as described in the *Materials and Methods* section. The CTL activities against ID8-T cells were analyzed in a standard ^{51}Cr-release assay using the indicated effector-to-target ratios. All determinations were made in triplicate samples, and the SD was <10%. Results are presented as the means ± SD of two independent experiments. $*P < 0.05$, $**P < 0.01$, $***P < 0.001$.

Table I

In vivo tumorigenicity of ID8 and ID8-T bulk cultures as well as $CD44^+$ and/or $CD117^+$ and double-negative subsets of ID8-T cells.

Cell type	Phenotype[a]	Injection site	Cell dose[c]	Tumor formation[d]	Latency days[e]
ID8	Bulk culture	s.c.	5×10^6	3/3	40/49/52
		s.c.	5×10^5	1/3	61
		i.p.	5×10^6	4/4	61/65/67/70
		i.p.[b]	5×10^6	3/3	63/68/72
ID8-T	Bulk culture	s.c.	5×10^5	3/3	24/29/32
		s.c.	2×10^4	2/3	37/39
		i.p.	5×10^6	3/3	24/28/35
		i.p.[b]	5×10^5	3/3	44/47/49
ID8-T	$CD44^+CD117^+$	s.c.	1×10^4	3/3	18/20/22
		s.c.	5×10^3	1/3	27
ID8-T	$CD44^-CD117^+$	s.c.	1×10^4	3/3	17/18/23
		s.c.	5×10^3	2/3	26/29
ID8-T	$CD44^+CD117^-$	s.c.	1×10^4	2/3	27/30
		s.c.	5×10^3	0/3	-
ID8-T	$CD44^-CD117^-$	s.c.	2×10^6	3/3	44/48/54
		s.c.	4×10^5	1/3	58
		s.c.	1×10^4	0/3	-

[a] Bulk cultures or ID8-T tumor cells sorted based on expression of CD44 and/CD117 antigens were injected s.c. or i.p. at different numbers to syngeneic C57BL/6 or SCID mice and monitored for tumor growth.

[b] Experiments were performed in SCID mice

[c] Number of cell per injection.

[d] Number of tumors per number of injection.

[e] The time from injection to the first appearance of a palpable tumor or ascites.